Tri-peptides on Gold Nanoparticles: Structural Differences Between Two Reverse Sequences as Determined by Solid-State NMR and DFT Calculations

ARTICLE *in* THE JOURNAL OF PHYSICAL CHEMISTRY B · AUGUST 2015

Impact Factor: 3.3 · DOI: 10.1021/acs.jpcb.5b04299 · Source: PubMed

6 AUTHORS, INCLUDING:

Ichhuk Karki

University of Pittsburgh

3 PUBLICATIONS **0** CITATIONS

SEE PROFILE

Hong Wang

West Virginia University

24 PUBLICATIONS **734** CITATIONS

SEE PROFILE

Brendan Wade Wilson

West Virginia University

1 PUBLICATION **0** CITATIONS

SEE PROFILE

James P Lewis

West Virginia University

90 PUBLICATIONS **2,796** CITATIONS

SEE PROFILE

THE JOURNAL OF PHYSICAL CHEMISTRY B

Article

pubs.acs.org/JPCB

Tripeptides on Gold Nanoparticles: Structural Differences between Two Reverse Sequences as Determined by Solid-State NMR and DFT Calculations

Ichhuk Karki,[†] Hong Wang,[‡] Natalie R. Geise,[†] Brendan W. Wilson,[†] James P. Lewis,[‡] and Terry Gullion*[,†]

[†]Department of Chemistry and [‡]Department of Physics and Astronomy, West Virginia University, Morgantown, West Virginia 26505, United States

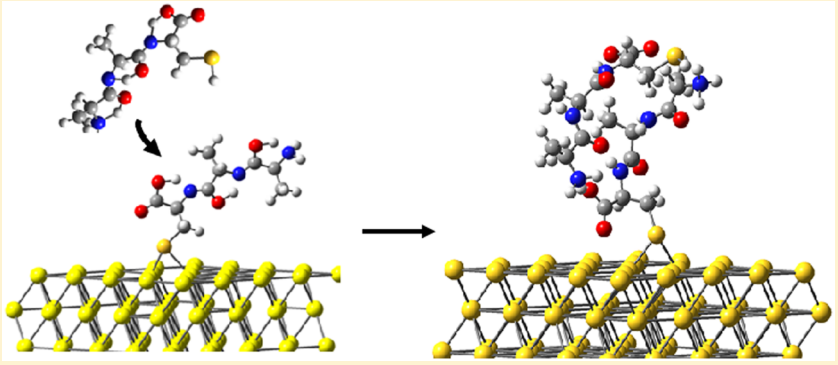

ABSTRACT: The reverse-sequence peptides CysAlaAla and AlaAlaCys may attach to gold nanoparticles through the thiol group, and they differ primarily by whether the charged amino or the carboxylate group is proximal to the sulfur. Alanine residues in these peptides are not expected to interact significantly with the gold surface and serve to place a large separation between the amino and carboxylate groups. Solid-state NMR experiments and DFT calculations were performed to explore the structural differences between CysAlaAla on gold nanoparticles and AlaAlaCys on gold nanoparticles. It is found that the relative positions between the thiol, amino, and carboxylate groups strongly influences the structures of the peptide−gold systems. CysAlaAla orients parallel to the gold surface in a monolayer fashion, whereas AlaAlaCys forms an interdigitating bilayer-like structure that is oriented upright relative to the gold surface.

I. INTRODUCTION

Self-assembly of biological molecules on metal nanoparticles has received considerable attention because of the potential applications, including imaging, drug delivery, and biosensors.[1−6] This interest has highlighted the need to understand the fundamental interactions and molecular structures at the interface. Solving molecular structures and characterizing molecule−metal interactions will provide better insight as to the functionality of the biomolecular−metal interface, which is critical for improving a variety of applications as well as for perceiving new applications.[7] However, the challenges to structural characterizations are immense because of the ability of the biomolecules to explore many conformations and the lack of crystalline materials.

One largely explored material for interfacing with biomolecules is gold nanoparticles. Gold nanoparticles have recently exhibited many promising properties for applications in biomedicine and biosensors.[8,9] For example, colloidal gold nanoparticles have emerged as preferable alternatives to other imaging dye agents because gold nanoparticles are believed to be nontoxic, exhibit facile immune-targeting, and are not susceptible to photobleaching or chemical and thermal denaturation, which are common issues associated with the dyes currently utilized.[10] Additionally, the X-ray and UV−vis absorption properties presented by biofunctionalized gold nanoparticles tend to be tunable by altering the nanoparticle's size and shape, which lends flexibility when engineering the optical properties based on a desired selectivity. Extensive studies have already shown that gold nanoparticles can be functionalized with biomolecules such as nucleic acids, peptides, or proteins, which are essential agents for designing bioimaging or treatment targets for specific parts of the body.

Cysteine is the only amino acid containing a thiol group that can bind strongly to either gold surfaces or gold nanoparticles; thus, it is an ideal linker to attach peptides and proteins to gold.[11−14] Furthermore, cysteine is an interesting molecule compared to the extensively studied alkanethiols on gold, especially considering the fact that cysteine may occur in a zwitterion form with charged amino and carboxyl groups that

Received: May 5, 2015
Revised: August 19, 2015

DOI: 10.1021/acs.jpcb.5b04299
J. Phys. Chem. B XXXX, XXX, XXX−XXX

lead to strong hydrogen-bonding networks that strongly influence structures.

Few structural options are possible for zwitterionic cysteine on gold nanoparticles because of the close proximity of the intramolecular carboxylate (COO^-) and amino (NH_3^+) groups.[15−22] As such, recent work suggests that cysteine forms a two-layer structure on gold nanoparticles with the inner layer chemisorbed through S−Au bonding and the outer layer stabilized to the inner layer through intermolecular salt bridges between the carboxylate and amino groups.[23−25] This perceived lack of structural diversity for cysteine on gold nanoparticles raises questions regarding the effects on molecular organization for cysteine-terminated peptides on gold nanoparticles where the intramolecular carboxylate−amino distances are large compared to the close spacing found in cysteine. We postulate that greater structural diversity is possible by placing the carboxylate and amino functional groups further apart, and that the structure will also depend on which of these terminal functional groups is nearest the thiol moiety.

A pair of reverse-sequence peptides were designed to explore the effect of large separations between the terminal amino and carboxylate groups on the structures of peptides interacting with gold nanoparticles. The peptides, CysAlaAla and AlaAlaCys, are identical in chemical composition while also having reverse amino acid sequences. Consequently, these peptides have different configurations of the aforementioned functional groups relative to the thiol group. The carboxylate carbon to amino nitrogen distances for the two peptides is around 9 to 10 Å for fully extended peptides. This distance range is noticeably longer than the corresponding 2.42 Å carbon−nitrogen distance in cysteine.[26] The thiol group of the cysteine residue provides the chemical attachment point to the gold surface, and the amino and carboxylate groups are free to interact with the gold surface or to form electrostatic interactions with their complementary counterparts. Alanine was chosen because its methyl group side chain does not interact with gold, does not participate in hydrogen bonding, and is not bulky. From this standpoint, the alanine residues were used as a spacer to separate the terminal carboxylate and amino groups in the zwitterionic peptides while keeping the peptides relatively simple. However, the alanine residues may assist in providing some structural diversity. For example, it is known that even the simple polyalanine tripeptide AlaAlaAla adopts either a parallel β sheet or antiparallel β sheet structure depending on sample preparation.[27,28]

We present solid-state NMR experiments and density functional theory calculations that show dramatic structural differences between CysAlaAla and AlaAlaCys on gold nanoparticles. The location of the carboxylate group relative to the sulfur atom that serves to anchor the peptide to the surface plays a major part in determining the structures.

II. EXPERIMENTAL METHODS AND COMPUTATIONAL PROCEDURES

Gold nanoparticles were prepared by reducing chloroauric acid using sodium borohydride. Typically, 100 mL of 1 mM $HAuCl_4$ solution was reduced by the dropwise addition of $NaBH_4$ (0.02 g total) and vigorously stirred for 1 h. Peptides were synthesized manually using FMOC solid-phase peptide synthesis on 2-C1-Trt resin. The peptides were purified by HPLC with a C18 semipreparative column (250 mm × 10 mm). The purity of the peptides was confirmed by solution ^{1}H NMR.

Peptide-coated gold nanoparticles were prepared by adding 3.68 mg of peptide to 10 mL of 1.9 mM HEPES buffer solution. This solution was then added to 90 mL of 1 mM gold nanoparticles and stirred slowly overnight under an argon atmosphere. The peptide-coated nanoparticles were recovered by centrifuging the solution at 15 000 rpm. Multiple washings of the recovered solid were performed to remove unbound peptide. The solid sample was lyophilized and stored in a freezer until needed. The peptide-coated nanoparticles were characterized by UV−vis and atomic force spectroscopy. Atomic force microscopy measurements of the recovered solid gave an average diameter of 12.4 ± 2.7 nm. UV−vis measurements taken before lyophilization showed a maximum absorbance at 518 nm, which is consistent with particle sizes in the 12 nm range.

Magic-angle spinning (MAS) NMR spectra were obtained on a custom-built spectrometer using a Tecmag Redstone console and a 3.55 T magnet (proton frequency of 151.395 MHz). The NMR probe is a transmission-line design, and it incorporates a Chemagnetics 7.5 mm pencil rotor spinning assembly with a 14 mm long, 8.65 mm inner diameter, 6 turn coil made of 14 gauge wire. Radio−frequency (rf) field strengths were 115 kHz for ^{1}H decoupling and 50 kHz for ^{1}H−^{13}C cross-polarization (CP).[29] The ^{1}H and ^{13}C power amplifiers were under active control. The spinning speed was set to 3125 Hz and actively controlled to within 0.2 Hz of the set point. All spectra were obtained with 1 s recycle delays and 1 ms matched Hartmann−Hahn cross-polarization transfers. The signal-to-noise ratios for the CPMAS spectra are low because of the poor filling factor associated with putting 10−20 mg of sample (most of which is gold and not peptide) in a 7.5 mm rotor assembly. There is also a noticeable ^{13}C background signal in the 90−170 ppm region arising from the stator parts located near the coil at this level of detection. This background signal could be eliminated by a simple echo sequence, but in the desire to minimize T_2 losses with such a small amount of sample and such a poor filling factor, only the standard ^{1}H−^{13}C CPMAS experiment was used in acquiring the NMR data.

Thermogravimetric analysis (TGA) was performed with a reconditioned PerkinElmer TGA 7 thermogravimetric analyzer. This particular TGA analyzer has a noticeable baseline drift, which is taken into account when analyzing the data. (The red dashed lines in Figures 4 and 5 represent the instrumental drift.) A similar instrumental drift was also observed with an empty pan. Mass corrections were made to account for the observed baseline drift.

Computational calculations were performed using the FIREBALL ab initio tight-binding package,[30] which is based on the density functional theory (DFT) with a nonlocal pseudopotential scheme. The two types of exchange-correlation density functionals in FIREBALL are LDA and GGA (BLYP) exchange.[31] The Becke exchange with the Lee−Yang−Parr exchange (BLYP) is known to provide reasonably good energy values for metal-containing systems and high levels of accuracy in the determination of a geometry optimization.[32] In our case, the adsorption structures and energies are our primary focus. Thus, we used the BLYP exchange for this study. The basis set is made of optimized numerical local atomic orbitals,[33,34] which were confined to regions limited by the corresponding cutoff radii r_c. The single numerical basis was chosen for hydrogen (H) with the radial cutoff value for the s-state orbital taken as $r_c^H(s) = 4.1$ au. A double numerical basis set was used for carbon (C), nitrogen (N), oxygen (O), and sulfur (S). The double

DOI: 10.1021/acs.jpcb.5b04299
J. Phys. Chem. B XXXX, XXX, XXX−XXX

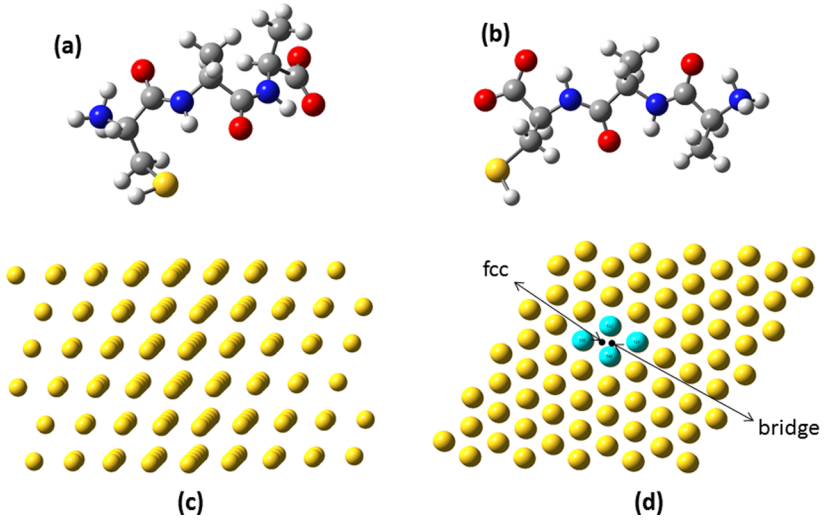

Figure 1. Optimized structures of CysAlaAla (a) and AlaAlaCys (b) peptides. The yellow balls represent S atoms, the red balls represent oxygen atoms, the blue balls represent nitrogen atoms, the white balls represent hydrogen atoms, and the gray balls represent carbon atoms. The left panel on the bottom, (c), is the optimized structure of the Au(111) surface (side view). We created a slab of the Au(111) surface with six layers. The right panel on the bottom, (d), is the top view of the optimized structure of Au(111). The four highlighted Au atoms illustrate potential attaching sites for the peptides.

numerical basis sets are generated by holding the ground-state wave-function fixed and exciting electron density to a higher orthogonal state with the same r_c value. Relevant cutoff radii are $r_c^C(s) = 4.3$ au, $r_c^C(p) = 4.7$ au, $r_c^N(s) = 3.9$ a. u., $r_c^N(p) = 4.4$ a. u., $r_c^O(s) = 3.6$ au, $r_c^O(p) = 4.0$ au, $r_c^S(s) = 4.5$ au, and $r_c^S(p) = 5.0$ au A polarized basis set sp^3d^5 obtained by adding a p-state orbital to the minimal basis set sd^5 was used for gold (Au). The gold cutoff radii are $r_c^{Au}(s) = 5.4$ au, $r_c^{Au}(p) = 5.8$ au, and $r_c^{Au}(d) = 5.0$ au. These basis sets have been successfully applied to a variety of systems, including DNA, zeolites, and metal oxides.[35−38]

The tendency of thin-film growth of gold to propagate in the [111] direction suggests that Au(111) has the lowest energy surface of gold.[39] Hence, the unreconstructed Au(111) surface was used to represent the Au nanoparticles in our calculations. Extensive studies have been devoted to the interaction between biomolecules and Au(111) surfaces.[40−44] Recent studies show that the bridge sites between Au atoms are the preferred adsorption sites for cysteine adsorption on the Au(111) surface.[31] (The simulation model in the referenced study[45] is three Au layers with a periodically repeated $(2\sqrt{3} \times 3)$ 2D supercell, corresponding to a surface area of 10.14×8.78 Å^2, and including 12 Au atoms per layer.) Since we are examining a tripeptide, we increased the size of the surface slab by using six Au layers with a periodically repeated (5×5) supercell. The surface area is ∼119 Å^2, which is sufficient enough to avoid significant interaction between the periodic images of the tripeptides. Along the z-direction, we set a 99 Å distance, which is large enough to separate the slabs. Several adsorption sites for the peptides are explored in this work, including bridge sites, fcc sites, and single-gold-atom sites. The two zwitterionic peptides and gold surfaces are shown in Figure 1.

III. RESULTS AND DISCUSSION

Cross-polarization magic-angle spinning (CPMAS)[29] NMR was used to characterize pure CysAlaAla and AlaAlaCys peptides and the peptides on 12 nm diameter gold nanoparticles. Because the three carbons of the cysteine residue were uniformly enriched with the ^{13}C isotope, the ^{13}C CPMAS NMR spectra are completely dominated by ^{13}C resonances from the cysteine residue of the two peptides.

Before proceeding with the presentation of the solid-state NMR results of the peptides, a brief description of previous ^{13}C CPMAS NMR results on L-cysteine on gold nanoparticles is provided and summarized in Table 1 to provide a point of reference.[23] A single ^{13}C resonance was observed for each of the carbon sites in a powder sample of L-cysteine. L-cysteine complexed with gold nanoparticles showed two sets of ^{13}C resonances for the $-CH_2$ and the $-CH$ carbons, which was indicative of two populations of cysteine. One set of resonances was shifted downfield by 12−15 ppm relative to pure L-cysteine, and the other set of resonances was found to be close to the original positions observed in pure L-cysteine. The downfield-shifted set was assigned to cysteine molecules forming an inner layer chemisorbed to the gold nanoparticles, and the unshifted set was assigned to an outer layer of cysteine molecules forming intermolecular salt bridges to the inner layer of cysteine.

Table 1. ^{13}C Isotropic Shifts for the ^{13}C Resonances Arising from Cysteine and the Cysteine Residue in the Peptides[a]

system	CH_2	CH	COO or C═O
Cys	28	54	173
Cys−Au	30 (2) and 43 (15)	54 (0) and 66 (12)	173 (0)
CysAlaAla	25	52	170
CysAlaAla−Au	53 (28)	71 (19)	184 (14)
AlaAlaCys	26	53	171
AlaAlaCys−Au	∼22 (−4) and 32 (6)	50 (−3) and 69 (16)	177 (6)

[a]Values are in parts per million (ppm) referenced to the ^{13}C resonance value of 20 ppm for the methyl group of simple L-alanine. The values in parentheses are the respective differences in the isotropic-shift values between the sample on gold and the pure sample (not on gold), and they are provided for convenience in illustrating the effect on isotropic shifts upon adding the sample to gold.

DOI: 10.1021/acs.jpcb.5b04299
J. Phys. Chem. B XXXX, XXX, XXX−XXX

The ^{13}C CPMAS NMR spectrum of AlaAlaCys on gold nanoparticles is shown in Figure 2. The blue lines mark the ^{13}C

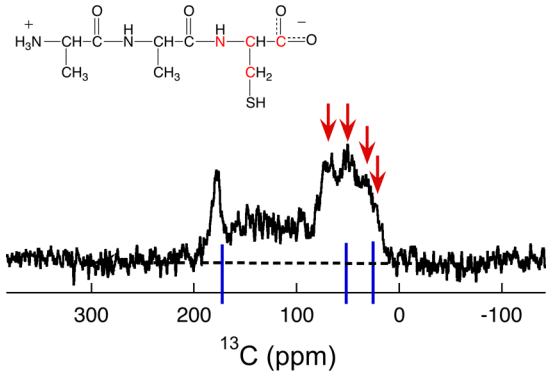

Figure 2. ^{13}C CPMAS spectrum of AlaAlaCys with uniform ^{13}C and ^{15}N labeling of the cysteine residue. The number of scans is 400 000. The signal-to-noise ratios for this spectrum and the one shown in Figure 3 are low because the small amount of samples are run in 7.5 mm rotors with corresponding very small filling factors. The zwitterion form of the peptide is shown, and the colored positions indicate isotopically enriched sites.

resonance positions for the three carbon sites of the C-terminus cysteine residue for pure AlaAlaCys (spectrum not shown) with their respective experimentally determined values provided in Table 1. The four arrows indicate two sets of ^{13}C resonances for the $-CH_2$ and $-CH$ carbon sites similar in features to those previously observed for cysteine on gold nanoparticles. The two more clearly identifiable peaks of similar intensities at 50 and 69 ppm arise from the $-CH$ carbon. This indicates the presence of two populations of peptide of comparable amounts. The two arrows indicating the peak at 32 ppm and the broad shoulder centered at 22 ppm are spectral features arising from the $-CH_2$ carbon. Comparing the isotropic shifts tabulated in Table 1 of pure peptide with those of the sample of peptide on gold shows that one set of ^{13}C resonances of AlaAlaCys on gold nanoparticles differs only slightly from the values observed for pure peptide, while the other set has resonance positions that are noticeably downfield-shifted. These features are similar to those observed for cysteine on gold nanoparticles and suggest that two populations of AlaAlaCys are present for the gold nanoparticle sample, with one population forming a chemisorbed layer on the gold surface and the other population most likely interacting with the chemisorbed peptide layer but not interacting strongly with the gold surface. There is only a single ^{13}C resonance for the $-COO$ carbon, suggesting that both peptide populations have similar environments for the carboxylate group.

The ^{13}C CPMAS NMR spectrum of CysAlaAla on gold nanoparticles is shown in Figure 3. The blue lines mark the ^{13}C resonance positions for the three carbon sites of the N-terminus cysteine residue for pure CysAlaAla (spectrum not shown), and their respective experimentally determined values are provided in Table 1. The arrows at 71 and 53 ppm indicate the ^{13}C resonances for the $-CH$ carbon and $-CH_2$ carbons, respectively. These resonance positions are downfield-shifted more strongly than either the cysteine or AlaAlaCys on gold nanoparticle samples. There appears to be only one set of ^{13}C resonances for this sample, suggesting that only one population of CysAlaAla is present. This is in marked contrast to the AlaAlaCys sample presented here and to the cysteine sample

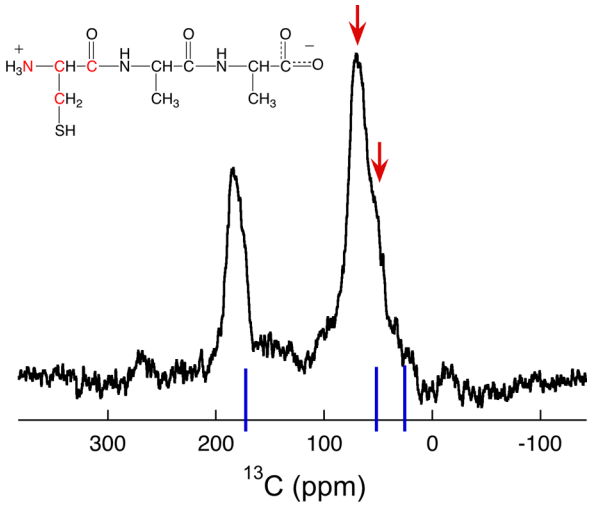

Figure 3. ^{13}C CPMAS spectrum of CysAlaAla with uniform ^{13}C and ^{15}N labeling of the cysteine residue. The number of scans for this spectrum is 400 000. The zwitterion form of the peptide is shown, and the colored positions indicate isotopically enriched sites.

reported earlier. In addition, the ^{13}C resonance of the cysteine carbonyl carbon is strongly shifted relative to pure peptide. The strong downfield shifts of all three ^{13}C resonances of the cysteine residue suggest a stronger interaction of the CysAlaAla peptide with the gold surface than that occurring for the AlaAlaCys and cysteine on gold samples.

Thermogravimetric analysis (TGA) was performed on the gold samples using a reconditioned PerkinElmer TGA 7 instrument. The TGA scan in Figure 4 shows the onset of desorption of AlaAlaCys on gold nanoparticles is approximately 135 °C, and the fractional loss of mass is 0.1573. The TGA scan

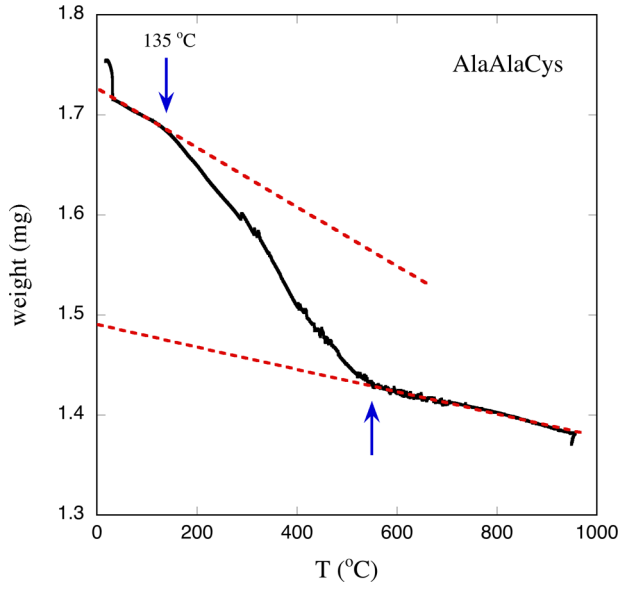

Figure 4. TGA plot of AlaAlaCys on 12.5 nm gold nanoparticles. The onset of peptide loss is 135 °C, as indicated by the left arrow. The temperature where desorption no longer occurs is indicated by the right arrow. For AlaAlaCys, the corrected total mass is 1.7264 mg, and the corrected mass of the gold is 1.4917 mg (from projections of the dashed lines representing baseline drift). Hence, the mass of AlaAlaCys is 0.2347 mg and the ratio of the mass of AlaAlaCys to gold is 0.1573.

DOI: 10.1021/acs.jpcb.5b04299
J. Phys. Chem. B XXXX, XXX, XXX−XXX

in Figure 5 shows the onset of desorption for CysAlaAla on gold nanoparticles is 266 °C, and its fractional loss of mass is

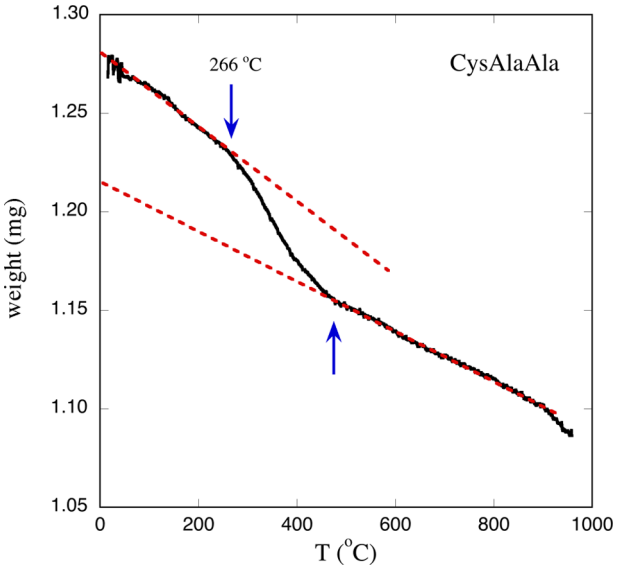

Figure 5. TGA plot of CysAlaAla on 12.5 nm gold nanoparticles. The onset of peptide loss is 266 °C, as indicated by the left arrow. The temperature where desorption no longer occurs is indicated by the right arrow. The corrected total mass is 1.2812 mg and the corrected mass of the gold is 1.2153 mg for the CysAlaAla sample, which gives 0.0659 mg of CysAlaAla and a mass ratio of peptide to gold of 0.0542.

0.0542. The two respective mass loss values show that there is 2.90 times as much AlaAlaCys than CysAlaAla on the gold nanoparticles, and that AlaAlaCys has a component (as evidenced by the lower desorption temperature) that is not as strongly bound as CysAlaAla.

Additional insights into the interactions of the two reverse-sequence peptides with gold nanoparticles were obtained by density functional theory calculations. The simulations used Au(111) because it has the lowest energy surface of gold and because recent studies show cysteine preferentially adsorbs at the bridge sites of the Au(111) surface.[24]

Figure 6 shows several configurations of CysAlaAla adsorbed on Au(111), along with their respective charge density differences, and specific details are provided in the figure caption. Inspection of the charge density differences along the peptides (aside from the thiol region) after adsorption shows that only small changes in charge density occur for four of the five geometries. However, a noticeable change in charge density is observed for the carboxylate group for the peptide with an orientation parallel to the surface. The additional attractive interaction between the terminal carboxylate group and the gold surface leads to the most energetically favorable orientation of the peptide. The charged carboxylate group at the C-terminus orients toward and is close to the Au surface, although there are no Au−O bonds formed. The surface orientation (parallel to the gold) of CysAlaAla is the most stable for a single molecule calculation. When another CysAlaAla is added to the system, it is found that a salt bridge forms between the $-NH_3^+$ of one CysAlaAla with the $-COO^-$ of the neighboring CysAlaAla peptide, which is illustrated in the bottom box of Figure 6 (corresponding energies listed in Table 2). In this manner, both peptides bind to the surface through their thiol groups and connect to each other via the intermolecular salt bridge. Considering the length of each CysAlaAla peptide in its nearly fully extended conformation, the peptides cover a relatively large surface area.

Figure 7 shows several configurations of AlaAlaCys adsorbed on Au(111) along with their respective charge density differences. It is clear from Figure 7 that the amino group stays away from the surface and that the charge density changes observed on the carboxylate group, which is proximal to the covalent S−Au attachment point, drives the upward orientation of the AlaAlaCys for all of the presented structures. In fact, because of the proximal nature of the carboxylate group to the S−Au position there is little variation in the overall energy between four of the five structures, which further suggests the importance the carboxylate group plays in determining the overall structure for both CysAlaAla and AlaAlaCys on gold. The DFT simulations find that the lowest adsorption energy occurs for a single AlaAlaCys peptide attaching at an fcc site and oriented in an upright fashion. We also find that AlaAlaCys does not interact with the Au surface as strongly as CysAlaAla. The upright orientation of AlaAlaCys leaves more gold surface area to accommodate, which potentially opens the way for more peptide to be associated with gold relative to the CysAlaAla system. When a second AlaAlaCys peptide is added to the system, it interacts with the original peptide by forming pairs of intermolecular NH_3^+ COO^- salt bridges, as shown in the bottom box of Figure 7.

The differences between the DFT structures of CysAlaAla and AlaAlaCys single peptides on gold arise from the relative positions between the thiolate and carboxylate groups of the respective peptides. The lowest energy structure of CysAlaAla on gold is −5.41 eV, while the lowest adsorption energy of AlaAlaCys on gold is −2.92 eV. These very different energies show stronger binding of CysAlaAla to gold than that for AlaAlaCys on gold. Au−S bond formation withdraws electron density from the gold, thereby providing a favorable condition for an electrostatic interaction between the gold surface and carboxylate ion. For CysAlaAla, this results in tilting the entire peptide toward the gold surface since the distal carboxylate group is far from the sulfur−gold attaching point. For AlaAlaCys, with its charged carboxylate group near the thiol group, the carboxylate attraction to the gold surface results in an upward tilting of the peptide about the sulfur anchor point away from gold surface.

IV. CONCLUDING REMARKS

The CPMAS NMR and TGA data along with the DFT calculations suggest the following models for CysAlaAla and AlaAlaCys on gold nanoparticles. A single layer of peptide chemisorbed to the gold surface via the thiol group and oriented roughly parallel to the surface is proposed for CysAlaAla. A single population of CysAlaAla was observed in the NMR experiments, with downfield-shifted ^{13}C resonances consistent with chemisorption. The TGA data shows a high onset temperature for desorption, presumably to overcome chemical bond attachment to the surface. The TGA data also finds less CysAlaAla on gold than that found for AlaAlaCys. If CysAlaAla is oriented parallel to the surface of gold, then less surface area is available for peptide attachment than if the peptide was oriented perpendicularly to the surface. The DFT calculations support a monolayer system with the CysAlaAla peptides lying more or less parallel to the surface and in a head-to-tail configuration with intermolecular salt bridges between the charged amino and carboxylate groups. The data and

DOI: 10.1021/acs.jpcb.5b04299
J. Phys. Chem. B XXXX, XXX, XXX−XXX

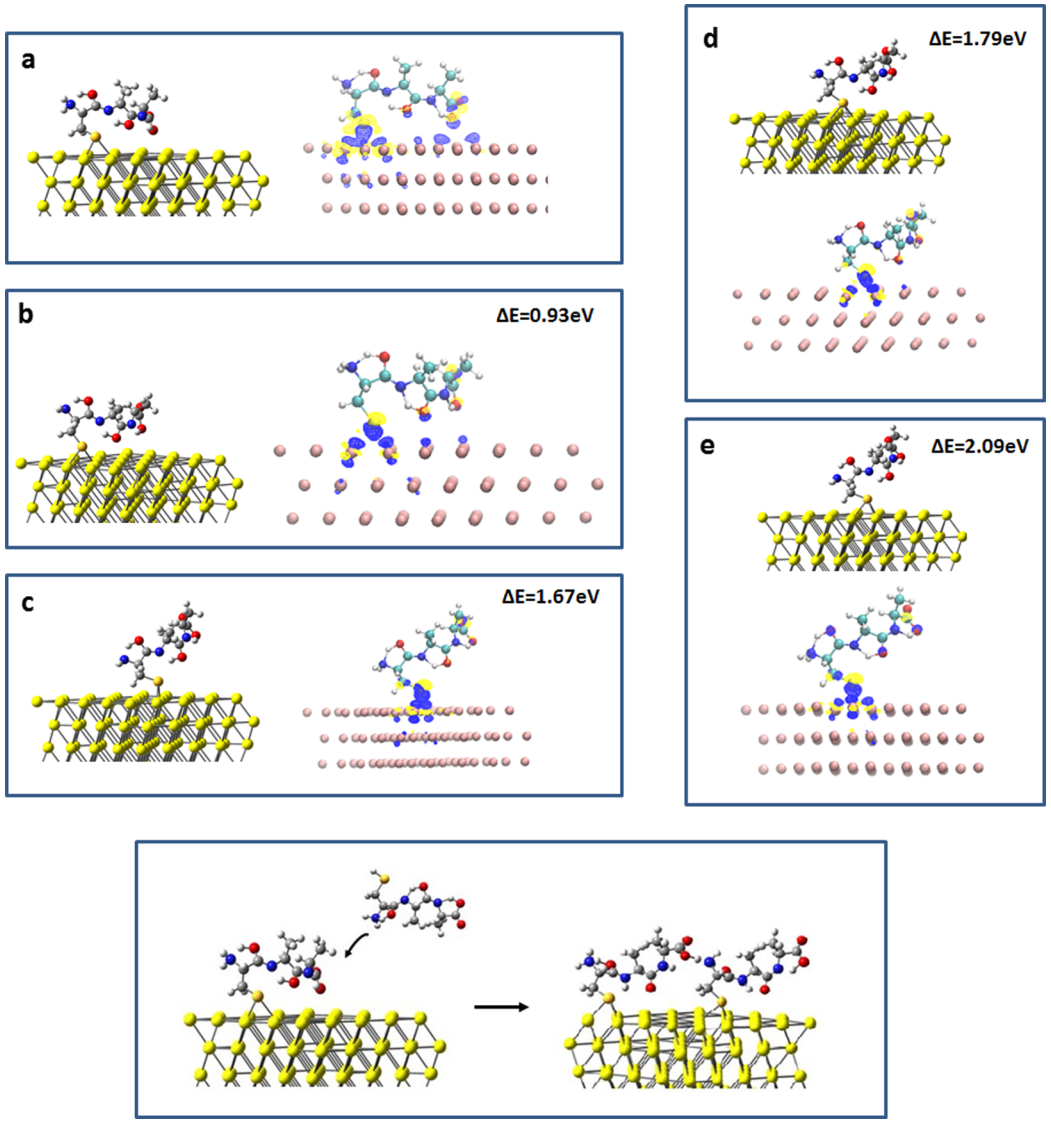

Figure 6. Representations of the five optimized attached structures of CysAlaAls on the Au(111) surface and the corresponding change in charge density contour images. The blue contour represents a charge-density increase, and the yellow contour represents a charge-density decrease (the contour value is set as 0.025). Panel a is bridge-parallel, panel b is bridge-tilting, panel c is bridge-upright, panel d is fcc-parallel, and panel e is fcc-upright. The corresponding energies are in Table 2. The relative energy is defined as the energy difference between structure energy *b* (or *c*, *d*, or *e*) and structure energy *a* ($\Delta E = b - a$, for instance). The bottom box illustrates the proposed attaching pattern when a second CysAlaAla peptide is added to the system.

Table 2. Adsorption Energies for Single Peptide (CysAlaAla and AlaAlaCys) Adsorption on Au(111) for Different Orientations of Peptide on the Gold Surface[a]

CysAlaAla configuration	CysAlaAla (eV)	AlaAlyCys configuration	AlaAlyCys (eV)
bridge-parallel	−5.41	fcc-parallel	−2.92
bridge-tilting	−4.48	fcc-upright	−2.84
bridge-upright	−3.74	bridge-parallel	−2.73
fcc-parallel	−3.62	bridge-upright	−2.49
fcc-upright	−3.32	bridge-tilting	−1.59

[a]The adsorption energy is defined as $E_{ads} = E_{complex} - E_{surface} - E_{peptide} + (1/2)E_{H_2}$. The structures for the tabulated configurations are shown in Figures 6 and 7.

calculations support an interdigitating model with the AlaAlaCys peptides oriented upward from the gold surface. One population of AlaAlaCys forms an inner layer chemisorbed to the gold surface, as evidenced by the set of cysteine residue ^{13}C resonances having downfield shifts. The second population of AlaAlaCys, which shows no downfield shifts of the ^{13}C resonances, forms pairs of intermolecular salt bridges to the chemisorbed layer and is not bonded to the surface. The TGA data showed a modest onset desorption temperature for AlaAlaCys, presumably because the outer layer is not as strongly held since it is not chemically attached to the surface. The TGA data finds more that twice the amount of AlaAlaCys is present compared to that in CysAlaAla. This is consistent with the upright orientation of the peptide found by DFT calculations, because an upright orientation frees more surface area for chemical attachment.

The reverse-sequence zwitterion peptides described in this work show distinctly different structures upon interacting with gold nanoparticles. This arises because of the large distance separation between the carboxylate and amino groups, and it

DOI: 10.1021/acs.jpcb.5b04299
J. Phys. Chem. B XXXX, XXX, XXX−XXX

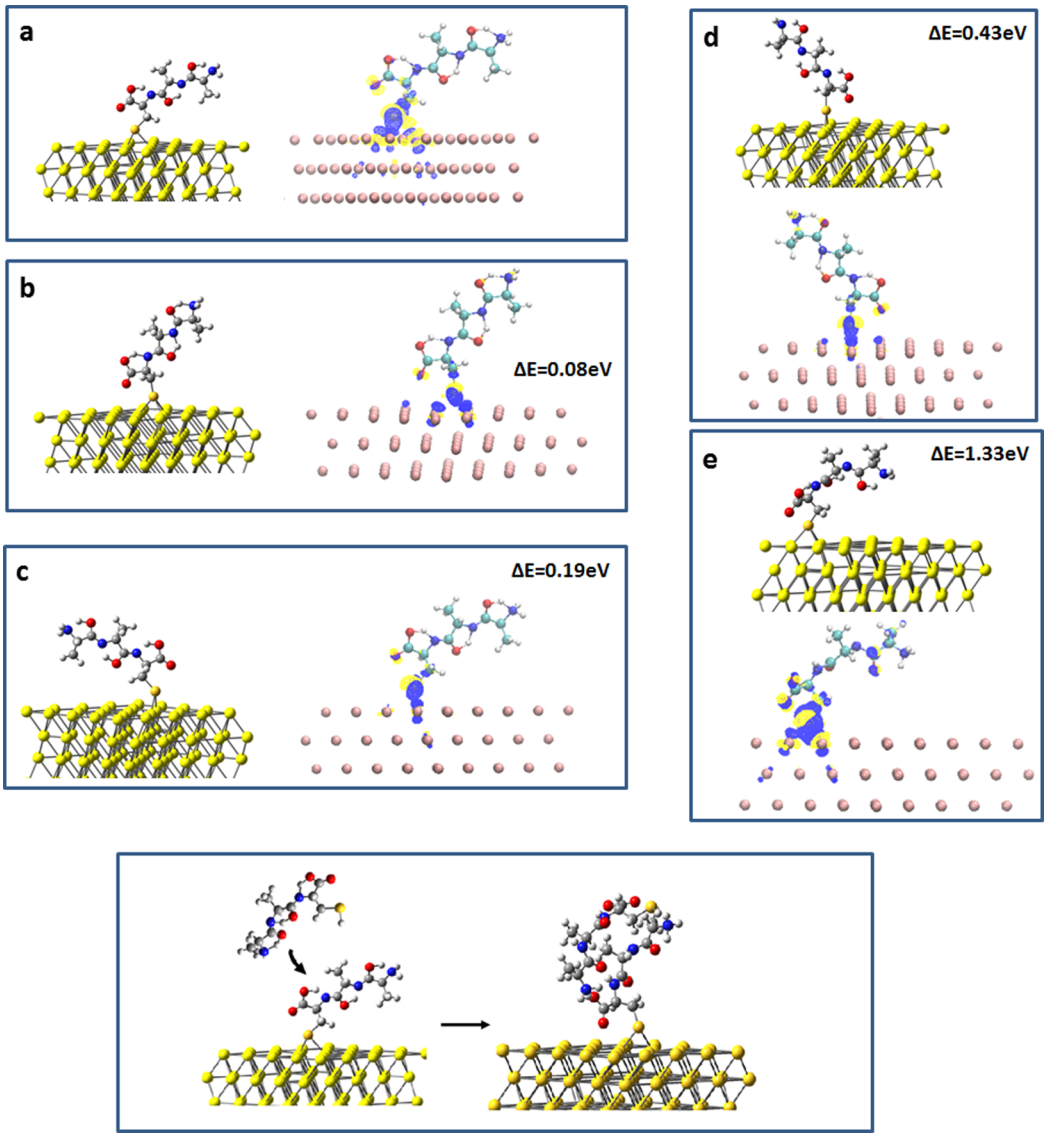

Figure 7. Representations of the five optimized attached structures of AlaAlaCys on the Au(111) surface and the corresponding change in charge density contour images. The blue contour represents a charge-density increase and the yellow contour represents a charge-density decrease (the contour value is set as 0.025). Panel a is fcc-parallel, panel b is fcc-upright, panel c is bridge-parallel, panel d is bridge-upright, and panel e is fcc-tilting. The corresponding energies are shown in Table 2. The relative energy is defined as the energy difference between structure energy *b* (or *c*, *d*, or *e*) and structure energy *a* ($\Delta E = b - a$, for instance). The bottom box illustrates the proposed interdigitating model when a second CysAlaAla peptide is added to the system.

matters which of these groups is near the thiol group. The AlaAlaCys and CysAlaAla peptides illustrate how the simple rearrangement of functional groups can influence structural aspects of peptides adsorbed on gold nanoparticles. Unlike alanine, many amino acids have side groups that can interact with gold surfaces, which suggests that further structural control of peptides at the surface can be had by appropriate choice of amino acid residues.

AUTHOR INFORMATION

Notes

The authors declare no competing financial interest.

ACKNOWLEDGMENTS

This work was supported by grants CHE-1152009 (T.G.) and CHE-1434378 (J.P.L.) from the National Science Foundation.

REFERENCES

(1) Huang, X.; El-Sayed, M. A. Gold Nanoparticles: Optical Properties and Implementations in Cancer Diagnosis and Photothermal Therapy. *J. Adv. Res.* **2010**, *1*, 13.

(2) Elghanian, R.; Storhoff, J. J.; Mucic, R. C.; Letsinger, R. L.; Mirkin, C. A. Selective Colorimetric Detection of Polynucleotides Based on the Distance-Dependent Optical Properties of Gold Nanoparticles. *Science* **1997**, *277*, 1078.

(3) Storhoff, J. J.; Elghanian, R.; Mucic, R. C.; Mirkin, C. A.; Letsinger, R. L. One-Pot Colorimetric Differentiation of Polynucleotides with Single Base Imperfections Using Gold Nanoparticle Probes. *J. Am. Chem. Soc.* **1998**, *120*, 1959.

(4) Frasconi, M.; Tortolini, C.; Botrè, F.; Mazzei, F. Multifunctional Au Nanoparticle Dendrimer-Based Surface Plasmon Resonance Biosensor and its Application for Improved Insulin Detection. *Anal. Chem.* **2010**, *82*, 7335.

DOI: 10.1021/acs.jpcb.5b04299
J. Phys. Chem. B XXXX, XXX, XXX−XXX

(5) Liu, J.; Xu, R.; Kaifer, A. E. In Situ Modification of the Surface of Gold Colloidal Particles. Preparation of Cyclodextrin-Based Rotaxanes Supported on Gold Nanospheres. *Langmuir* **1998**, *14*, 7337.
(6) Zhang, C.; Zhang, Z.; Yu, B.; Shi, J.; Zhang, X. Application of the Biological Conjugate Between Antibody and Colloid Au Nanoparticles as Analyte to Inductively Coupled Plasma Mass Spectrometry. *Anal. Chem.* **2002**, *74*, 96.
(7) Vallee, A.; Humblot, V.; Pradier, C.-M. Peptide Interactions with Metal and Oxide Surfaces. *Acc. Chem. Res.* **2010**, *43*, 1297.
(8) Pingarrón, J. M.; Yáñez-Sedeño, P.; González-Cortés, A. Gold Nanoparticle-Based Electrochemical Biosensors. *Electrochim. Acta* **2008**, *53*, 5848.
(9) Saha, K.; Agasti, S. S.; Kim, C.; Li, X.; Rotello, V. M. Gold Nanoparticles in Chemical and Biological Sensing. *Chem. Rev.* **2012**, *112*, 2739.
(10) Li, Y.; Schluesener, H.; Xu, S. Gold Nanoparticle-Based Biosensors. *Gold Bulletin* **2010**, *43*, 29.
(11) Chi, Q.; Zhang, J.; Nielsen, J. U.; Friis, E. P.; Chorkendorff, I.; Canters, G. W.; Andersen, J. E. T.; Ulstrup, J. Molecular Monolayers and Interfacial Electron Transfer of Pseudomonas Aeruginosa Azurin on Au(111). *J. Am. Chem. Soc.* **2000**, *122*, 4047.
(12) Baas, T.; Gamble, L.; Hauch, K. D.; Castner, D. G.; Sasaki, T. Characterization of a Cysteine-Containing Peptide Tether Immobilized onto a Gold Surface. *Langmuir* **2002**, *18*, 4898.
(13) Nitzan, A.; Ratner, M. A. Electron Transport in Molecular Wire Junctions. *Science* **2003**, *300*, 1384.
(14) Gerster, D.; Reichert, J.; Bi, H.; Barth, J. V.; Kaniber, S. M.; Holleitner, A. W.; Visoly-Fisher, I.; Sergani, S.; Carmeli, I. Photocurrent of a Single Photosynthetic Protein. *Nat. Nanotechnol.* **2012**, *7*, 673.
(15) Uvdal, K.; Bodo, P.; Liedberg, B. L-Cysteine Adsorbed on Gold and Copper: An X-Ray Photoelectron Spectroscopy Study. *J. Colloid Interface Sci.* **1992**, *149*, 162.
(16) Kuhnle, A.; Linderoth, T. R.; Hammer, B.; Besenbacher, F. Chiral Recognition in Dimerization of Adsorbed Cysteine Observed by Scanning Tunneling Microscopy. *Nature* **2002**, *415*, 891.
(17) Kuhnle, A.; Linderoth, R. R.; Schunack, M.; Besenbacher, F. L-Cysteine Adsorption Structures on Au(111) Investigated by Scanning Tunneling Microscopy under Ultrahigh Vacuum Conditions. *Langmuir* **2006**, *22*, 2156.
(18) Cossaro, A.; Terreni, S.; Cavalleri, O.; Prato, M.; Cvetko, D.; Morgante, A.; Floreano, L.; Canepa, M. Electronic and Geometric Characterization of the L-Cysteine Paired-Row Phase on Au(110). *Langmuir* **2006**, *22*, 11193.
(19) Filimon, A.-D.; Jacob, P.; Hergenroder, R.; Jurgensen, A. Study on the Reversible Changes of the Surface Properties of an L-Cysteine Self-Assembled Monolayer on Gold as a Function of pH. *Langmuir* **2012**, *28*, 8692.
(20) Tawil, N.; Hatef, A.; Sacher, E.; Maisonneuve, M.; Gervais, T.; Mandeville, R.; Meunier, M. Surface Plasmon Resonance Determination of the Binding Mechanisms of L-Cysteine and Mercaptoundecanoic Acid on Gold. *J. Phys. Chem. C* **2013**, *117*, 6712.
(21) Honda, M.; Baba, Y.; Hirao, N.; Sekiguchi, T. Observation of Au-S Interface of L-Cysteine on Gold Surface. *e-J. Surf. Sci. Nanotechnol.* **2009**, *7*, 110.
(22) Honda, M.; Baba, Y.; Hirao, N.; Sekiguchi, T. Metal-Molecular Interfaces of Sulfur-Containing Amino Acid and Thiophene on Gold Surface. *J. of Phys.: Conference Series* **2008**, *100*, 052071.
(23) Abraham, A.; Mihaliuk, E.; Kumar, B.; Legleiter, J.; Gullion, T. Solid-State NMR Study of Cysteine on Gold Nanoparticles. *J. Phys. Chem. C* **2010**, *114*, 18109.
(24) Abraham, A.; Iliot, A. J.; Miller, J.; Gullion, T. ^{1}H MAS NMR Study of Cysteine-coated Gold Nanoparticles. *J. Phys. Chem. B* **2012**, *116*, 7771.
(25) Carr, J.; Wang, H.; Abraham, A.; Gullion, T.; Lewis, J. P. L-Cysteine Interaction with Au_{55} Nanoparticle. *J. Phys. Chem. C* **2012**, *116*, 25816.
(26) Harding, M. M.; Long, H. A. The Crystal and Molecular Structure of L-Cysteine. *Acta Crystallogr., Sect. B: Struct. Crystallogr. Cryst. Chem.* **1968**, *B24*, 1096.
(27) Hempel, A.; Camerman, N.; Camerman, A. L-Alanyl-L-Alanyl-L-Alanine: Parallel Pleated Sheat Arrangment in Unhydrated Crystal Structure, and Comparisons with the Antiparallel Sheet Structure. *Biopolymers* **1991**, *31*, 187.
(28) Fawcett, J. K.; Camerman, N.; Camerman, A. The Structure of the Tripeptide L-Alanyl-L-Alanyl-L-Alanine. *Acta Crystallogr., Sect. B: Struct. Crystallogr. Cryst. Chem.* **1975**, *31*, 658.
(29) Schaefer, J.; Stejskal, E. O. Carbon-13 Nuclear Magnetic Resonance of Polymers Spinning at the Magic Angle. *J. Am. Chem. Soc.* **1976**, *98*, 1031.
(30) Lewis, J. P.; Jelínek, P.; Ortega, J.; Demkov, A. A.; Trabada, D. G.; Haycock, B.; Wang, H.; Adams, G.; Tomfohr, J. K.; Abad, E.; et al. Advances and Applications in the Fireball *Ab Initio* Tight-binding Molecular-dynamics Formalism. *Phys. Status Solidi B* **2011**, *248*, 1989−2007.
(31) Jelínek, P.; Wang, H.; Lewis, J. P.; Sankey, O. F.; Ortega, J. Multicenter Approach to the Exchange-correlation Interactions in *Ab Initio* Tight-binding Methods. *Phys. Rev. B: Condens. Matter Mater. Phys.* **2005**, *71*, 235101.
(32) Grönbeck, H.; Curioni, A.; Andreoni, W. Thiols and Disulfides on the Au(111) Surface: The Headgroup-Gold Interaction. *J. Am. Chem. Soc.* **2000**, *122* (16), 3839−3842.
(33) Sankey, O. F.; Niklewski, D. J. *Ab Initio* Multicenter Tight-binding Model for Molecular-Dynamics Simulations and Other Applications in Covalent Systems. *Phys. Rev. B: Condens. Matter Mater. Phys.* **1989**, *40*, 3979−3995.
(34) Sankey, O. F.; Demkov, A. A.; Windl, W.; Fritsch, J. H.; Lewis, J. P.; Fuentes-Cabrera, M. The Application of Approximate Density Functionals to Complex Systems. *Int. J. Quantum Chem.* **1998**, *69*, 327−340.
(35) Lewis, J. P.; Ordejon, P.; Sankey, O. F. Electronic-structure-based Molecular-dynamics Method for Large Biological Systems: Application to the 10 Basepair Poly(dG)·Poly(dC) DNA Double Helix. *Phys. Rev. B: Condens. Matter Mater. Phys.* **1997**, *55*, 6880−6887.
(36) Wang, H.; Lewis, J. P. The Reactive Sites in Faceted Anatase Nanoparticles. *Phys. Status Solidi B* **2011**, *248*, 2037−2043.
(37) Wang, L.; Wang, H.; Zhang, W.; Zhang, J.; Lewis, J. P.; Meng, X. J.; Xiao, F. S. Aerobic Homocoupling of Phenylboronic Acid on Mg-Al Mixed-oxides-supported Au Nanoparticles. *J. Catal.* **2013**, *298*, 186−197.
(38) Wu, N. Q.; Wang, J.; Tafen, D. N.; Wang, H.; Zheng, J. G.; Lewis, J. P.; Liu, X. G.; Leonard, S. S.; Manivannan, A. Shape-Enhanced Photocatalytic Activity of Single-Crystalline Anatase TiO_2 (101) Nanobelts. *J. Am. Chem. Soc.* **2010**, *132*, 6679−6685.
(39) Valden, M.; Lai, X.; Goodman, D. W. Onset of Catalytic Activity of Gold Clusters on Titania with the Appearance of Nonmetallic Properties. *Science* **1998**, *281*, 1647.
(40) Huang, X.; El-Sayed, M. A. Gold nanoparticles: Optical Properties and Implementations in Cancer Diagnosis and Photothermal Therapy. *J. Adv. Res.* **2010**, *1*, 13−28.
(41) Vallée, A.; Humblot, V.; Pradier, C. M. Peptide Interactions with Metal and Oxide Surfaces. *Acc. Chem. Res.* **2010**, *43*, 1297−1306.
(42) Vallée, A.; Humblot, V.; Méthivier, C.; Pradier, C. M. Adsorption of a Tripeptide, GSH, on Au(111) under UHV Conditions; PM-RAIRS and Low T-XPS Characterisation. *Surf. Sci.* **2008**, *602*, 2256−2263.
(43) Vallée, A.; Humblot, V.; Méthivier, C.; Pradier, C. M. Glutathione Adsorption from UHV to the Liquid Phase at Various pH on Gold and Subsequent Modification of Protein Interaction. *Surf. Interface Anal.* **2008**, *40*, 395−399.
(44) Vallée, A.; Humblot, V.; Méthivier, C.; Pradier, C. M. Adsorption of Di- and Tripeptides on Au(110) under Ultrahigh Vacuum Conditions. 1. Polarization Modulation Reflection Absorption Infrared Spectroscopy and X-ray Photoelectron Spectroscopy Characterization. *J. Phys. Chem. C* **2009**, *113*, 9336−9344.

DOI: 10.1021/acs.jpcb.5b04299
J. Phys. Chem. B XXXX, XXX, XXX−XXX

(45) Di Felice, R.; Selloni, A.; Molinari, E. DFT Study of Cysteine Adsorption on Au(111). *J. Phys. Chem. B* **2003**, *107*, 1151−1156.

DOI: 10.1021/acs.jpcb.5b04299
J. Phys. Chem. B XXXX, XXX, XXX−XXX